ISCoS The International Spinal Cord Society

www.nature.com/sc

ARTICLE

Check for updates

DTI of chronic spinal cord injury in children without MRI abnormalities (SCIWOMR) and with pathology on MRI and comparison to severity of motor impairment

Scott H. Faro[1]✉, Sona Saksena[1], Laura Krisa[2,3], Devon M. Middleton[1], Mahdi Alizadeh[4], Jürgen Finsterbusch[5], Adam E. Flanders[1], Kiran Talekar[1], M. J. Mulcahey[3] and Feroze B. Mohamed[1]

STUDY DESIGN: This investigation was a cohort study that included: 36 typically developing (TD) children and 19 children with spinal cord lesions who underwent spinal cord MRI.
OBJECTIVES: To investigate diffusion tensor imaging (DTI) cervical and thoracic spinal cord changes in pediatric patients that have clinically traumatic and non-traumatic spinal cord injury (SCI) without MR (SCIWOMR) abnormalities.
SETTING: Thomas Jefferson University, Temple University, Shriners Hospitals for Children all in Philadelphia, USA.
METHODS: 36 TD children and 19 children with spinal cord lesions that represent either a chronic traumatic acquired SCI or chronic non-traumatic SCI (≥6 months post injury), age range, 6–16 years who underwent cervical and thoracic spinal cord MRI in 2014–2017. Additionally DTI was correlated to clinical American Spinal Injury Association Impairment Scale (AIS).
RESULTS: Both SCIWOMR and MRI positive (+) groups showed abnormal FA and RD DTI values in the adjacent MRI-normal appearing segments of cephalad and caudal spinal cord compared to TD. The FA values demonstrated perilesional abnormal DTI findings in the middle and proximal segments of the cephalad and caudal cord in the SCIWOMR AIS A/B group compared to SCIWOMR AIS C/D group.
CONCLUSIONS: We found DTI changes in children with SCIWOMR with different causes of spinal lesions. We also investigated the relationship between DTI and clinical AIS scores. This study further examined the potential diagnostic value of DTI and should be translatable to adults with spinal cord lesions.

Spinal Cord (2022) 60:457–464; https://doi.org/10.1038/s41393-022-00770-5

INTRODUCTION

In children, spinal cord lesions are due to a variety of traumatic and non-traumatic causes. With reference to trauma, the term spinal cord injury (SCI) without radiographic abnormality (SCIWORA) has been used primary in children with SCI that do not show any plain film radiographic abnormality. SCIWORA was originally described by Pang and Wilberger as a traumatic myelopathy without evidence of injury on plain radiographs [1]. SCIWORA is relatively common in children with SCI. In this population it comprises nearly 20% of children under the age of 3 years and 9.4% of children aged 3 to 12 years, whereas for individuals aged 12–20 years, the incidence decreases to 5% [2]. The injury is thought to occur due to the increased elasticity of the pediatric cervical vertebral column in comparison to the spinal cord and the relatively large head-to-body ratio in young children [3, 4].

SCI can be categorized into two types of injury: primary injury, which is the consequence of the initial trauma or impact of force; and secondary injury, which occurs as a complication of secondary insults following primary injury [5]. In individuals with SCI, secondary injury may involve the development of necrosis, glial scarring and cavitation. These secondary injuries develop through a multi-factorial process, including infiltration of astrocytes, microglia, macrophages, fibroblasts [6, 7], chemokines and their receptors [8] as well as chronic axonal injury such as Wallerian degeneration [9]. These processes interfere with spinal cord recovery by preventing axonal regeneration and also the associated inflammatory response can itself cause injury [10]. Under these circumstances, examining the tissue distant from the injury site with DTI, including the corticospinal tract in the brain and cervical cord above the lesion may provide valuable insights into spinal cord function [11]. Studies have also showed DTI and cross-sectional imaging findings that correlated to remote secondary neurodegeneration cord pathology below the level of spinal cord injury [12]. Others have also shown that the neurodegenerative processes of the brain and spine are related and demonstrated imaging correlates of brain and cord atrophy, myelin content and thalamic iron accumulation changes over time in SCI [13].

[1]Department of Radiology, Thomas Jefferson University, 909 Walnut Street, Philadelphia, PA 19107, USA. [2]Department of Occupational Therapy, Thomas Jefferson University, 901 Walnut Street, 6th floor, Philadelphia, PA 19107, USA. [3]Department of Physical Therapy, Thomas Jefferson University, 901 Walnut Street, 5th floor, Philadelphia, PA 19107, USA. [4]Department of Neurosurgery, Thomas Jefferson University, 909 Walnut Street, Philadelphia, PA 19107, USA. [5]University Medical Center, Hamburg-Eppendorf, Hamburg, Germany. ✉email: scott.faro@jefferson.edu

Received: 13 January 2021 Revised: 16 December 2021 Accepted: 4 February 2022
Published online: 4 April 2022

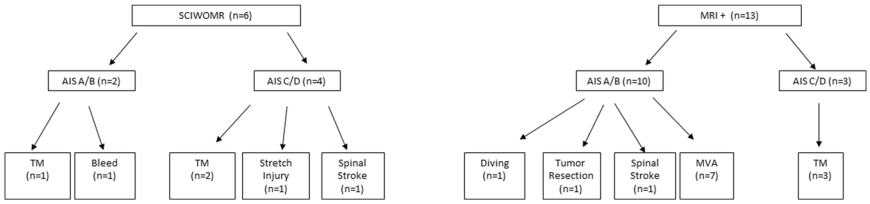

Fig. 1 Breakdown of etiology between participants in the two groups: SCIWOMR and MRI+ The two groups include spinal cord injury without MR abnormnalities (SCIWOMR) and spinal cord injury with positive MR findings (MRI+). Each group is also separated into two clinical subgroups: AIS A/B and AIS C/D and associated etiology/pathology.

Imaging of the spine has added important information to the medical care of individuals, although radiology studies may not show abnormalities. For example computerized tomography (CT) scanning may not demonstrate spinal cord abnormality in individuals with SCI, referred to SCI without CT evidence of trauma (SCIWOCTET) [14]. The use of MRI has further advanced imaging of SCI and many other spinal cord pathologic processes due to the ability to better characterize spinal canal and intramedullary abnormalities Fig. 1. Although conventional magnetic resonance imaging (MRI) has been used to evaluate the spinal cord parenchyma and provides anatomical information it has limited sensitivity to detect more subtle changes that occur at a distance away from the primary SCI.

In 10% of SCI no MRI abnormality is identified [15]. In addition to routine MRI, advanced functional MRI techniques such as diffusion-tensor imaging (DTI) has long thought to have capacity to further identify abnormalities in individuals without MRI findings [16]. DTI provides microstructural information and has been capable of detecting pathology beyond the primary spinal cord lesion in regions that appear normal on standard MRI sequences [17, 18]. Our group has focused our research on the use of advanced MRI techniques using DTI, as a potential biomarker in the pediatric population with SCI and has shown changes in the spinal cord white matter regions remote from the lesion [19, 20]. Others have described the term SCI without neuroimaging abnormality (SCIWNA) that includes MRI [21]. We have also found that some pediatric individuals have a clinical diagnosis of a spinal cord abnormality, however, do not demonstrate any lesion on a routine MRI. Although it is clear that clinically, MRI is currently the best imaging modality to characterize intramedullary pathology [22], we propose a more specific term that describes individuals that have clinically a spinal cord lesion without abnormalities seen on MRI as spinal cord injury without MRI findings (SCIWOMR). Previously, our group and others have demonstrated in individuals with SCI that have a focal spinal cord lesion on MRI have abnormal DTI changes in normal appearing spinal cord above and below the lesion shown on MRI [19, 23–25,]. We will referrer to participants with a focal spinal cord lesion on a routine structural MRI as MRI+. This study will use advanced MRI using DTI to investigate spinal cord changes in pediatric individuals with SCIWOMR in addition to individuals with a variety of intramedullary pathology on MRI. Additionally, we and others think that DTI will potentially correlate to the clinical score in individuals with SCI, as measured by the American Spinal Injury Association Impairment Scale (AIS) [19, 26]. Specifically, in pediatric participant groups with an AIS scores of A or B (motor complete) would be compared to participant groups with some motor function, an AIS score of C or D (motor incomplete).

While there are limited studies (ref) on SCIWORA in the adult SCI population,to the best of our knowledge, there have been no previous studies using DTI to examine children with SCIWOMR, with clinically diagnosed spinal cord lesions and correlated DTI to clinical AIS scores. This will further examine the potential diagnostic value of DTI in these participant groups and should also be translatable to adults with spinal cord lesions.

METHODS

Study design

This study was part of a larger investigation to examine the feasibility of DTI for pediatric SCI [19, 27]. All participants were volunteers and recruited for the purpose of research. The current study included 36 typically developing (TD) children (age range, 6–16 years; mean age, 11.72 ± 3.12; 15 males (M) and 21 females (F) and 19 children with spinal cord lesions that represent either a chronic traumatic acquired SCI or chronic non-traumatic SCI (=> 6 months post injury, age range, 6–16 years; mean age, 12.16 ± 2.91; 9 M and 10 F) who underwent spinal cord imaging in 2014–2017. Table 1 shows the demographic information of the children with SCI as defined by conventional MRI. SCI participants were classified into two subgroups of varying severity based on the type of spinal cord lesion seen on anatomic MRI, SCIWOMR ($n = 6$) and MRI positive (+) ($n = 13$).

Prior to scanning, the participant's level and severity of injury was accurately determined by undergoing a complete International Standards for Neurological Classification of Spinal Cord Injury (ISNCSCI) examination by a trained therapist [26]. This examination consisted of the following components. Sensory testing consisted of testing 28 dermatomes on each side of the body for sensitivity to sharp-dull discrimination (via Pin Prick (PP) testing) and Light Touch (LT). At a specified point in each dermatome, sensitivity to PP and LT was evaluated and scored using the three-point scale consisting of "0" (absent), "1" (impaired) and "2" (unimpaired). Motor examination was completed through the manual strength testing of ten key muscles bilaterally. The strength of each muscle was graded on a six-point ordinal scale between "0" (complete paralysis) to "5" (normal active movement, full range of motion against full resistance). The anorectal examination was performed to evaluate deep anal pressure (DAP) and contraction of the external anal sphincter (AC). Participants were classified according to their neurological function below the level of the lesion: AIS A – absence of motor and sensory function; AIS B – absence of motor function, but some degree of preserved sensation below the injury; AIS C/D – some preserved motor and sensory function below the injury. The lesion location in individuals with SCIWOMR ($n = 6$) was based on the neurological level (NL) of injury as defined by the ISNCSCI score. In participant 205 the MRI of the spine was degraded by motion artifact with no gross lesion identified. The second participant group had spinal cord abnormalities on MR imaging (defined as MRI positive (+) ($n = 13$) that included participants with syringohydromyelia ($n = 2$), atrophy + syringomyelia ($n = 5$), atrophy + myelomalacia ($n = 3$) and atrophy + hemorrhage ($n = 3$) (Table 1). Written informed child assent and parent consent were obtained under the protocol approved by the Institutional Review Board.

Inclusion criteria for the TD participants were: no evidence of abnormal spinal cord pathology as assessed by performing a neurologic screen and a brief assessment of motor and sensory function and reflexes. Inclusion criteria for spinal cord lesion participants: stable spinal cord lesion in the past 3 months and were at least 6 months post diagnosis of a spinal cord lesion. Exclusion criteria for all participants: unable to tolerate MR imaging without sedation or; any abnormality (unrelated to the SCI) of the nervous and/or musculoskeletal system; orthodontic hardware or other internal metal material.

Imaging acquisition

A 3 T MR scanner (Siemens, Germany) with a 4-channel neck matrix and an 8-channel spine matrix coil was used. Conventional T1- and T2-weighted MRI scans were obtained for all the participants. The T2-weighted image of the cervical and thoracic spinal cord in the sagittal plane was initially obtained using a gradient echo (GRE) sequence and was used to facilitate slice prescription for the subsequent scans perpendicular to the cord. Next, an axial GRE T2-weighted, sagittal T2-weighted 3D SPACE, sagittal turbo

Table 1. Demographic Information of the SCI Subjects.

Subject ID	Age at Enrollment (years)	Gender	Cephalad and caudal margins of the lesion present on MRI *based on NL	NL	AIS grade	MRI Findings	Etiology
115	9.24	M	*MC5-MC6	C6	B	SCIWOMR	TM
205	9.42	F	*MT8-MT9	T9	A	SCIWOMR	Bleed
206	8.07	F	*C1-MD	C1	D	SCIWOMR	TM
207	13.72	M	*C4-C5/C5-C6	C5	D	SCIWOMR	Stretch injury
210	12.37	M	*C1-MD	C1	D	SCIWOMR	TM
142	13.96	F	T11-T12/MT12	L2	C	SCIWOMR	Spinal stroke
216	7.03	F	MT12/T12-L1	L2	D	Syringomyelia	TM
129	9.99	F	C4-C5	C5	D	Syringomyelia +/− Myelomalacia	TM
217	16.99	M	MC3-MC4	C4	B	Atrophy + Syringomyelia	Diving
215	14.96	M	MC6/T1-T2	C8	A	Atrophy + Syringomyelia	MVA
204	12.65	F	C6-C7/CONUS	T3	A	Atrophy + Syringomyelia	MVA
203	11.04	F	MT5-MT8	T4	A	Atrophy + Syringomyelia	Tumor resection
221	14.13	F	C6-C7/MT6	T3	B	Atrophy + Syringomyelia	MVA
212	12.68	M	T10-T11	T12	A	Atrophy + Myelomalacia	MVA
208	8.08	M	MC6/C7-T1	C8	A	Atrophy + Myelomalacia	MVA
118	15.15	F	MT10-MT12	T10	B	Atrophy + Myelomalacia	Spinal stroke
209	15.71	M	T8-T9/CONUS	T9	A	Atrophy + Hemorrhage	MVA
201	11.12	M	C5-C6/MT5	C6	A	Atrophy + Hemorrhage	MVA
219	14.88	F	T2-T3/T4-T5	T4	D	Atrophy + Hemorrhage	TM

MRI magnetic resonance imaging, *M* male, *F* female, *M* mid, *NL* neurological level, *AIS* American Spinal Injury Association Impairment Scale, *SCIWOMR* spinal cord without MRI findings, *TM* transverse myelitis, *MVA* motor vehicle accident.
*Based on NL.

Table 2. Summary of changes of FA and RD in segments of the cord cephalad and caudal to the level of MRI lesion in SCI participants with SCIWOMR ($n = 6$) and TD participants ($n = 36$).

DTI Metrics	Subjects	Cephalad			Caudal		
		Distal	Middle	Proximal	Proximal	Middle	Distal
FA	TD	0.595 ± 0.090	0.583 ± 0.075	0.534 ± 0.090	0.545 ± 0.093	0.595 ± 0.097	0.515 ± 0.115
	SCIWOMR	0.603 ± 0.070	**0.471 ± 0.093** ⇩ $p < 0.0001$	0.509 ± 0.128	**0.472 ± 0.092** ⇩ $p = 0.0002$	**0.481 ± 0.078** ⇩ $p < 0.0001$	**0.456 ± 0.099** ⇩ $p = 0.0028$
RD	TD	0.625 ± 0.180	0.674 ± 0.149	0.731 ± 0.222	0.590 ± 0.214	0.629 ± 0.260	0.575 ± 0.252
	SCIWOMR	0.667 ± 0.149	**0.743 ± 0.205** ⇧ $p = 0.0444$	0.717 ± 0.301	**0.811 ± 0.163** ⇧ $p < 0.0001$	**0.828 ± 0.150** ⇧ $p < 0.0001$	**0.754 ± 0.226** ⇧ $p < 0.0001$

Bold indicates significantly different DTI value in SCI subjects with SCIWOMR compared to TD subjects.

spin-echo (TSE) T1-weighted, sagittal TSE T2-weighted and axial DTI scans using an inner field of view (iFOV) sequence were obtained for the participants. The iFOV sequence used in this study has been described in detail elsewhere [28]. Manual shim volume adjustments were also performed prior to data acquisition in order to restrict the adjustment volume to the anatomy of interest in an effort to further improve the signal.

The iFOV sequence was optimized for both signal and scan duration to image the entire pediatric cervical and thoracic spinal cord. DTI scans were acquired axially in the same anatomical location prescribed for the T2-weighted gradient echo images to cover the cervical (C1-upper thoracic region) and thoracic (upper thoracic-L1) spinal cord using two overlapping slabs [19]. The imaging parameters for each slab of DTI acquisition included: field of view, 164 mm; phase field of view, 47 mm; number of excitations, 3; number of diffusion directions, 20; b0 images, 6; *b* value, 800 s/mm^2; voxel, $0.8 \times 0.8 \times 6$ mm^3; axial slices, 40; repetition time, 7900 ms; echo time, 110 ms; and acquisition time, 8:49 min. To shorten the amount of time the participants were in the scanner anesthesia and cardiac and respiratory gating were not used.

Data pre-processing

A central mask was applied to the raw DTI images to eliminate the anatomy outside the spinal cord. Motion correction was performed first on the 6 b0 images to create a mean b0 image and the diffusion weighted images were subsequently co-registered to the mean b0 image [29]. The diffusion data sets were corrected for motion induced artifacts based on 3D registration technique using an in-house software developed in Matlab (MathWorks, Natick, Massachusetts) [29]. The technique uses rigid body transformation with 6 degrees of freedom (3 translational, 3 axis rotations) paired with normalized mutual information as cost function to align target images (20 diffusion directional images) with the reference image (b0). A robust, iterative diffusion tensor estimation scheme, RESTORE, was implemented to ensure removal of data outliers from the final tensor fit [30]. All processing in this study was performed using previously developed and published techniques [19]. At the time of study inception, these were not all readily available as pre-built software, particularly for spinal cord applications. In the intervening time, publicly available/open source implementations of these have become more common and the same techniques used in this paper can be performed easily using these implantations.

Region of interest analysis

Regions of interest (ROIs) were drawn manually on axial fractional anisotropy (FA) maps to extract the whole cord along the cervical and thoracic spinal cord. ROI was drawn at each intervertebral disk and mid-vertebral body level of the cervical and thoracic spinal cord to compute DTI metrics FA, mean diffusivity (MD), axial diffusivity (AD) and radial diffusivity (RD). There was a consistent sparring of the outer margin of the spinal cord of approximately one voxel width to minimize volume averaging with cerebrospinal fluid. These ROIs were anatomically localized by a board-certified pediatric neuroradiologist using axial T2-weighted gradient echo images as a reference. For each SCI participant, the cephalad and caudal regions of the normal appearing spinal cord were separated into three equal segments: proximal third, middle third and distal third cephalad and caudal to the level of lesion on MRI as previously described [19]. We did not include the injured cord as this would likely cause spurious results. TD cord for comparison was chosen based on the epicenter as the average of the spinal cord lesion in each SCI group. For SCIWOMR group, epicenter was mid T1, C1 to C7-T1 was defined as the cephalad spinal cord and T1-T2 to T12-L1 was defined as the caudal spinal cord and for MRI+ group, epicenter was mid T5, C1 to T4-T5 was defined as the cephalad spinal cord and T5-T6 to T12-L1 was defined as the caudal spinal cord. In the group analysis of six segments of the entire cord (three cephalad and three caudal), TD cord was separated into proximal third, middle third and distal third and compared to the respective segments in the SCI participants in each SCIWOMR and MRI+ group. Additionally, we performed similar analysis between TD cord and SCI participants divided into AIS grades A/B (motor complete) and C/D (motor incomplete) in each SCIWOMR and MRI + group for both cephalad and caudal cord. The SCIWOMR group had two SCI participants with AIS grade A/B and four SCI participants with AIS grade C/D and MRI+ had ten SCI participants with AIS grade A/B and three SCI participants with AIS grade C/D respectively (Table 1).

Statistical analysis

Statistical analysis was performed using JMP pro 13.0 software. The data were checked for normality using Shapiro-Wilk test and the data were not normally distributed. To detect differences in DTI metrics between the normal appearing spinal cord in TD participants and normal appearing spinal cord for SCI participants in SCIWOMR and MRI+ groups was further divided into AIS grades A/B and C/D, a nonparametric Wilcoxon test was performed respectively. A $p < 0.05$ was used for statistical significance.

RESULTS

In the following tables the double bars indicates the region of the spinal cord lesion that is not included in the data analysis and lies between the proximal cephalad and caudal (peri-lesional) regions. Group analysis is of segments of the spinal cord cephalad and caudal to the clinical level of a cord lesion in individuals with SCIWOMR and MRI+ groups compared to TD participants.

Both SCIWOMR and MRI+ groups showed abnormal DTI values in the adjacent MRI-normal appearing segments of cephalad and caudal spinal cord compared to TD. FA was significantly decreased ($p < 0.05$) whereas RD was significantly increased ($p < 0.05$) in the proximal, middle and distal segments of the caudal cord on comparing TD to SCI participants with SCIWOMRIn the middle segment of the cephalad cord, FA was significantly ($p < 0.0001$) decreased while RD was significantly ($p = 0.0444$) increased. There was more abnormality found in the caudal cord compared to cephalad cord as shown by decreased FA (Caudal_Proximal: $p = 0.0002$; Caudal_Middle: $p < 0.0001$; Caudal_Distal: $p = 0.0028$) and increased RD (Caudal_Proximal: $p < 0.0001$; Caudal_Middle: $p < 0.0001$; Caudal_Distal: $p < 0.0001$) in all three caudal divisions (Table 2). We found a significant decrease in FA in all segments of the cephalad (Cephalad_Distal: $p = 0.0235$; Cephalad_Middle: $p < 0.0001$; Cephalad_Proximal: $p < 0.0001$) and caudal cord (except for distal segment) (Caudal_Proximal: $p < 0.0001$; Caudal_Middle: $p < 0.0001$) on comparing TD to SCI participants with MRI+. RD was significantly increased in all segments of the cephalad (except for distal segment) (Cephalad_Middle: $p = 0.0242$; Cephalad_Proximal: $p < 0.0001$) and caudal cord (Caudal_Proximal: $p = 0.0435$; Caudal_Middle: $p = 0.0141$; Caudal_Distal: $p = 0.0277$) (Table 3).

Table 3. Summary of changes of FA and RD in segments of the cord cephalad and caudal to the level of MRI lesion in SCI subjects with MRI+ ($n = 13$) and TD subjects ($n = 36$).

DTI Metrics	Subjects	Cephalad			Caudal		
		Distal	Middle	Proximal	Proximal	Middle	Distal
FA	TD	0.593 ± 0.085	0.551 ± 0.088	0.537 ± 0.091	0.595 ± 0.100	0.574 ± 0.100	0.503 ± 0.120
	SCI-MRI+	**0.554 ± 0.122** ⇩ $p = 0.0235$	**0.492 ± 0.108** ⇩ $p < 0.0001$	**0.447 ± 0.120** ⇩ $p < 0.0001$	**0.394 ± 0.102** ⇩ $p < 0.0001$	**0.477 ± 0.119** ⇩ $p < 0.0001$	0.460 ± 0.097
RD	TD	0.643 ± 0.174	0.706 ± 0.200	0.593 ± 0.215	0.665 ± 0.269	0.592 ± 0.247	0.545 ± 0.240
	SCI-MRI +	0.730 ± 0.287	**0.777 ± 0.237** ⇧ $p = 0.0242$	**0.909 ± 0.461** ⇧ $p < 0.0001$	**0.774 ± 0.322** ⇧ $p = 0.0435$	**0.683 ± 0.261** ⇧ $p = 0.0141$	**0.633 ± 0.228** ⇧ $p = 0.0277$

Bold indicates significantly different DTI value in SCI participants with MRI+ compared to TD participants.

Table 4. Summary of changes of FA and RD in segments of the cord cephalad and caudal to the level of MRI lesion in SCI subjects with SCWOMR (S) categorized into AIS groups A/B ($n = 2$) and C/D ($n = 4$) and TD subjects ($n = 36$).

DTI Metrics	Subjects	Cephalad			Caudal		
		Distal	Middle	Proximal	Proximal	Middle	Distal
FA	TD	0.595 ± 0.090	0.583 ± 0.075	0.534 ± 0.090	0.545 ± 0.093	0.595 ± 0.097	0.515 ± 0.115
	SCIWOMR A/B	0.609 ± 0.081	**0.476 ± 0.082** ⇩ $p < 0.0001$	**0.437 ± 0.068** ⇩ $p = 0.0004$	**0.422 ± 0.034** ⇩ $p < 0.0001$	**0.510 ± 0.075** ⇩ $p = 0.0107$	0.445 ± 0.104
	SCIWOMR C/D	0.597 ± 0.061	**0.468 ± 0.105** ⇩ $p < 0.0001$	0.581 ± 0.134	0.494 ± 0.101	**0.474 ± 0.078** ⇩ $p < 0.0001$	**0.459 ± 0.099** ⇩ $p = 0.0113$
RD	TD	0.625 ± 0.180	0.674 ± 0.149	0.731 ± 0.222	0.590 ± 0.214	0.629 ± 0.260	0.575 ± 0.252
	SCIWOMR A/B	0.698 ± 0.159	**0.780 ± 0.133** ⇧ $p = 0.0159$	**0.895 ± 0.116** ⇧ $p = 0.0010$	**0.776 ± 0.16** ⇧ $p = 0.00672$	0.730 ± 0.112	**0.847 ± 0.144** ⇧ $p = 0.0008$
	SCIWOMR_C/D	0.639 ± 0.138	0.711 ± 0.252	**0.539 ± 0.328** ⇩ $p = 0.0466$	**0.825 ± 0.165** ⇧ $p < 0.0001$	**0.853 ± 0.150** ⇧ $p < 0.0001$	**0.730 ± 0.238** ⇧ $p = 0.0013$

Bold indicates significantly different DTI value in SCI subjects with SCIWOMR compared to TD subjects. Red indicates a discordant value of DTI metric.

Group analysis of segments of the cord cephalad and caudal to the lesion comparing SCI-SCIWOMR and MRI+AIS grades (A/B, C/D) to TD

SCIWOMR DTI findings in AIS A/B verses AIS C/D. The FA values demonstrated perilesional abnormal DTI findings in the middle and proximalsegments of the cephalad (Cephalad_Middle: $p < 0.0001$; Cephalad_Proximal: $p = 0.0004$) and caudal cord (Caudal_Proximal: $p < 0.0001$; Caudal_Middle: $p = 0.0107$) in the SCIWOMR AIS A/B compared to the TD group. In SCIWOMR AIS C/D compared to the TD group there were cephalad changes in the proximal segment ($p < 0.0001$) and middle ($p = 0.0107$) and proximal ($p < 0.0001$) segments of the caudal cord (Table 4). In reviewing RD data, there were perilesional RD changes in the cephalad middle ($p = 0.0159$) and proximal ($p = 0.0010$) cord and caudal proximal ($p = 0.00672$) and distal ($p = 0.0008$) cord in SCIWOMR AIS A/B group. In the RD SCIWOMR AIS C/D group a discordant RD-DTI value in the proximal cephalad ($p = 0.0466$) cord was demonstrated (noted in red) in comparison to the FA data which does not demonstrate any discordant DTI values. Additionally, there were changes in all three caudal segments (Caudal_Proximal: $p < 0.0001$; Caudal_Middle: $p < 0.0001$; Caudal_Distal: $p = 0.0013$) (Table 4).

MRI+DTI findings in AIS A/B verses AIS C/D. The FA values demonstrated abnormal perilesional DTI findings in both the MRI + AIS A/B (Cephalad_Middle: $p = 0.0070$; Cephalad_Proximal: $p < 0.0001$; Caudal_Proximal: $p < 0.0001$; Caudal_Middle: $p = 0.0014$) and C/D (Cephalad_Distal: $p < 0.0001$; Cephalad_Middle: $p < 0.0001$; Cephalad_Proximal: $p < 0.0001$; Caudal_Proximal: $p < 0.0001$; Caudal_Middle: $p < 0.0001$) groups compared to TD (Table 5). When compared to the TD group, the RD data showed only perilesional abnormal DTI changes in the MRI + A/B group (Cephalad_Proximal: $p < 0.0001$; Caudal_Proximal: $p = 0.0267$), however, there were a greater number of abnormal spinal cord segments in the MRI + C/D group (Cephalad_Distal: $p < 0.0001$; Cephalad_Middle: $p < 0.0001$; Cephalad_Proximal: $p < 0.0001$; Caudal_Middle: $p = 0.0042$) (Table 5).

Comparison of SCIWOMR to MRI+DTI findings. When comparing FA DTI values of the SCIWOMR to MRI+, we found the perilesional FA abnormality in the proximal caudal spinal cord (Table 6). RD showed abnormal DTI values in the middle and distal caudal segments (Table 6).

DISCUSSION

Significant FA and RD DTI changes were manifested in the adjacent MRI-normal appearing spinal cord cephalad and caudal to the neurologic level of that correlates to a lesion in SCIWOMR or abnormal cord signal on MR imaging in the MRI+ group. These findings suggest that DTI can capture microstructural changes distant from a neurologic level in individuals with SCIWOMR that is not evident on conventional MRI. To the best of our knowledge, this is the first study showing significant DTI alterations in the cephalad and caudal cord of pediatric individuals with SCIWOMR.

A previous MRI study showed a low energy traumatic thoracic SCIWORA after a back bend during dance practice in children younger than 8 years old ($n = 12$, mean age: 6.6 years). It is theorized that significant longitudinal distraction of the thoracic spine during the back bend causes the forced lengthening of the thoracic cord and leads to axonal disruption and neural cell membrane breakage [31]. This study however does not describe

Table 5. Summary of changes of FA and RD in segments of the cord cephalad and caudal to the level of MRI lesion in SCI subjects with MRI+ categorized into AIS groups A/B ($n = 10$) and C/D ($n = 3$) and TD subjects ($n = 36$).

DTI Metrics	Subjects	Cephalad			Caudal		
		Distal	Middle	Proximal	Proximal	Middle	Distal
FA	TD	0.593 ± 0.085	0.551 ± 0.088	0.537 ± 0.091	0.595 ± 0.100	0.574 ± 0.100	0.503 ± 0.120
	SCI-MRI + _A/B	0.593 ± 0.109	**0.510 ± 0.105** ⇩ $p = 0.0070$	**0.454 ± 0.126** ⇩ $p < 0.0001$	**0.383 ± 0.094** ⇩ $p < 0.0001$	**0.497 ± 0.126** ⇩ $p = 0.0014$	0.462 ± 0.076
	SCI- MRI + _C/D	**0.441 ± 0.079** ⇩ $p < 0.0001$	**0.441 ± 0.105** ⇩ $p < 0.0001$	**0.426 ± 0.102** ⇩ $p < 0.0001$	**0.414 ± 0.118** ⇩ $p < 0.0001$	**0.432 ± 0.090** ⇩ $p < 0.0001$	0.455 ± 0.138
RD	TD	0.643 ± 0.174	0.706 ± 0.200	0.593 ± 0.215	0.665 ± 0.269	0.592 ± 0.247	0.545 ± 0.240
	SCI- MRI + _A/B	0.635 ± 0.245	0.729 ± 0.227	**0.882 ± 0.509** ⇧ $p < 0.0001$	**0.798 ± 0.298** ⇧ $p = 0.0267$	0.642 ± 0.276	0.617 ± 0.174
	SCI- MRI + _C/D	**0.999 ± 0.221** ⇧ $p < 0.0001$	**0.914 ± 0.214** ⇧ $p < 0.0001$	**0.987 ± 0.273** ⇧ $p < 0.0001$	0.728 ± 0.371	**0.776 ± 0.205** ⇧ $p = 0.0042$	0.669 ± 0.328

Bold indicates significantly ($p < 0.05$) different DTI value in SCI subjects with MRI+ compared to TD subjects.

Table 6. Summary of changes of FA and RD in segments of the cord cephalad and caudal to the level of MRI lesion in SCI subjects with MRI+ ($n = 13$) and SCIWOMR ($n = 6$).

DTI Metrics		Cephalad			Caudal		
		Distal	Middle	Proximal	Proximal	Middle	Distal
FA	MRI+	0.554 ± 0122	0.492 ± 0.108	0.447 ± 0.120	0.394 ± 0.102	0.477 ± 0.119	0.460 ± 0.097
	SCIWOMR	0.603 ± 0.070	0.471 ± 0.093	0.509 ± 0.128	**0.472 ± 0.092** ⇧ $p = 0.0019$	0.481 ± 0.078	0.456 ± 0.099
RD	MRI+	0.730 ± 0.287	0.777 ± 0.237	0.909 ± 0.461	0.774 ± 0.322	0.683 ± 0.261	0.633 ± 0.228
	SCIWOMR	0.667 ± 0.149	0.743 ± 0.205	0.717 ± 0.301	0.811 ± 0.163	**0.828 ± 0.150** ⇧ $p = 0.0007$	**0.754 ± 0.226** ⇧ $p = 0.0231$

Bold indicates significantly ($p < 0.05$) different DTI values in MRI+ compared to SCIWOMR.

the MRI findings in their SCIWORA group. In our SCIWOMR group both FA and RD in the entire caudal cord were statistically abnormal with normal DTI in the proximal cephalad cord suggesting Wallerian axonal degeneration. Abnormal FA and RD was also seen in the middle cephalad cord consistent with a degree of retrograde degeneration. These DTI changes represented a variety of etiologies including one participant with a stretch injury.

Quantitative DTI metrics have been confirmed previously in experimental models to reflect a variety of histopathological changes in the chronic spinal injury setting including myelomalacia, gliosis, cavitation, Wallerian degeneration and demyelination [18, 32, 33]. Our findings of decreased FA and increased RD values observed in the segments of the cephalad and caudal cord in SCIWOMR and MRI+ individuals are consistent with DTI changes in animal models [18, 32].

The pattern of perilesional abnormal DTI metrics may give us insight into the severity and full extent of spinal cord abnormality in individuals with spinal cord lesions. We define perilesional abnormal DTI metrics as a minimum of both proximal cephalad and proximal caudal segments with abnormal DTI values compared to TD spinal cord. Overall, the most extensive perilesional abnormal DTI values were seen in the FA and RD metrics in the MRI+ participants.

We also investigated if there was a correlation between the severity of spinal cord lesions as determined by subsets of AIS scores (AIS A/B vs C/D) and DTI. Due to the small number of participants in each AIS grade, AIS A and AIS B were grouped together given they are both motor complete injuries. Likewise AIS C and AIS D were grouped together since they are both motor incomplete injures. We found that in SCIWOMR AIS A/B group, FA demonstrated perilesional abnormal DTI findings in the segments of the cephalad and caudal cord, however SCIWOMR AIS C/D group did not show perilesional FA abnormality. This shows that the severity of disease may correlate to the abnormality seen on DTI when comparing SCIWOMR AIS group A/B to the less severe SCIWOMR AIS C/D group. This suggests that as the severity of injury increases, FA becomes more isotropic i.e., there are less barriers to water movement. The RD DTI changes theoretically relate to an increase in radial diffusivity due to a loss of restriction of water movement orthogonal to the long axis of the axon due to demyelination. In the SCIWOMR AIS A/B group there were perilesional RD abnormalities cephalad and caudal to the lesion consistent with both anterograde and retrograde degeneration. Only concordant RD abnormality was seen in the caudal spinal cord of the SCIWOMR AIS C/D group. This is consistent with more global cord abnormality in the SCIWOMR AIS A/B group in comparison to only anterograde degeneration in the SCIWOMR AIS C/D group. This also suggests there may be a correlation between AIS scores and DTI metrics.

Review of the FA changes in the MRI + AIS A/B groups showed similar abnormal DTI changes in the cephalad and caudal spinal cord to the MRI + C/D group and the SCIWOMR AIS A/B group. This suggests that there may be a greater correlation of AIS scores to FA DTI changes in the SCIWOMR group. When the FA chances were compared between MRI+ and SCIWOMR groups five out of the six regions showed no significant changes. However, the proximal caudal segments were statistically different. Both regions had a FA values that were lower than the FA of subjects in the TD group, however, the SCIWOMR group was less abnormal compared to the MRI+ group. This may suggest that the MRI+ group had a greater degree of injury leading to more FA changes.

One of the limitations of the study is the low number of SC lesion participants in the SCIWOMR group ($n = 6$). Although the n is low for the SCIWOMR participants, we wanted to look at the proportion of abnormal DTI values in relation to the severity of injury and because of this we separated the participants into two groups, SCIWOMR A/B ($n = 2$) and SCIWOMR C/D ($n = 4$). Future work with large number of participants with spinal cord lesions with different AIS categories would be important to further assess the DTI differences in the cord of children with SCIWOMR and MRI+ participants. Another limitation is the use of manual ROI selection, which may have introduced partial volume contamination from the cerebrospinal fluid surrounding the cord. The ROIs drawn were conservative, to minimize this volume-averaging effect. Cardiac gating is known to improve image quality, however, this requires increased imaging time. Given this is a pediatric study we felt it was important to minimize the time the participant spent in the scanner.

We demonstrated the utility of quantitative DTI analysis to better characterize the extent of severity of pathologic damage in different segments of the spinal cord cephalad and caudal to the lesion in pediatric SCI participants with SCIWOMR and MRI+ compared to TD participants. DTI was able to detect changes in the cephalad and caudal cord of SCIWOMR participants whereas MRI could not. These DTI results might provide valuable information about selecting treatment strategies and facilitate in the prognostic evaluation of SCIWOMR and MRI+ individuals.

DATA AVAILABILITY

Raw data is available upon request assuming a data sharing agreement can be executed.

REFERENCES

1. Pang D. Spinal cord injury without radiographic abnormality in children, 2 decades later. Neurosurgery.2004;55:1325–43.
2. Piatt JH. Pediatric spinal injury in the US: epidemiology and disparities. J Neurosurg—Pediatr. 2015;16:463–71.
3. Osenback RK, Menezes AH. Spinal cord injury without radiographic abnormality in children. Pediatr Neurosurg. 1989;15:168–75.
4. Pang D. Spinal cord injury without radiographic abnormality in children. In: Betz RR, Mulcahey MJ The child with a spinal cord injury. Rosemont, IL: American Academy of Orthopedic Surgeons. 1996;168–75.
5. Oyinbo CA. Secondary injury mechanisms in traumatic spinal cord injury: a nugget of this multiply cascade. Acta Neurobiol Exp. 2011;71:281–99.
6. Jones LL, Margolis RU, Tuszynski MH. The chondroitin sulfate proteoglycans neurocan, brevican, phosphacan, and versican are differentially regulated following spinal cord injury. Exp Neurol. 2003;182:399–411.
7. Schultz SS. Adult stem cell application in spinal cord injury. Curr Drug Targets. 2005;6:63–73.
8. Knerlich-Lukoschus F, Held-Feindt J. Chemokine-ligands/receptors: multiplayers in traumatic spinal cord injury. Mediators Inflamm. 2015;2015:486758.
9. Cohen-Adad J, Leblond H, Delivet-Mongrain H, Martinez M, Benali H, Rossignol S. Wallerian degeneration after spinal cord lesions in cats detected with diffusion tensor imaging. Neuroimage. 2011;57:1068–76.
10. Schwartz ED, Duda J, Shumsky JS, Cooper ET, Gee J. Spinal cord diffusion tensor imaging and fiber tracking can identify white matter tract disruption and glial scar orientation following lateral funiculotomy. J Neurotrauma. 2005;22:1388–98.
11. Freund P, Schneider T, Nagy Z, Hutton C, Weiskopf N, Friston K, et al. Degeneration of the injured cervical cord is associated with remote changes in corticospinal tract integrity and upper limb impairment. PLoS ONE. 2012;7:e51729 https://doi.org/10.1371/journal.pone.0051729
12. David G, Seif M, Huber E, Hupp M, Rosner J, Dietz V, et al. In vivo evidence of remote neural degeneration in the lumbar enlargement after cervical injury. Neurology.2019;92:e1367–77.
13. Ziegler G, Grabher P, Thompson A, Altmann D, Hupp M, Ashburner J, et al. Progressive neurodegeneration following spinal cord injury: Implications for clinical trials. Neurology.2018;90:e1257–66.
14. Como JJ, Samia H, Nemunaitis GA, Jain V, Anderson JS, Malangoni MA, et al. The misapplication of the term spinal cord injury without radiographic abnormality (SCIWORA) in adults. J Trauma Acute Care Surg. 2012;73:1261–6.
15. Boese CK, Lechler P. Spinal cord injury without radiologic abnormalities in adults: a systematic review. J Trauma Acute Care Surg. 2013;75:320–30.
16. Shen H, Tank Y, Huang L, et al. Applications of diffusion-weighted MRI in thoracic spinal cord injury without radiographic abnormality. Int Orthop. 2007;31:375–83.
17. Sundberg LM, Herrera JJ, Narayana PA. In vivo longitudinal MRI and behavioral studies in experimental spinal cord injury. J Neurotrauma. 2010;27:1753–67.
18. Ellingson BM, Schmit BD, Kurpad SN. Lesion growth and degeneration patterns using diffusion tensor 9.4-T magnetic resonance imaging in rat spinal cord injury. J Neurosurg Spine. 2010;13:181–92.
19. Saksena S, Mohamed FB, Middleton DM, Krisa L, Alizadeh M, Shahrampour S. DTI Assessment of Regional White Matter Changes in the cervical and thoracic spinal cord in pediatric participants. J Neurotrauma. 2019;19:853–61.
20. Conklin CJ, Middleton DM, Alizadeh M, Finsterbusch J, Raunig DL, Faro SH, et al. Spatially selective 2D RF inner field of view (iFOV) diffusion kurtosis imaging (DKI) of the pediatric spinal cord. Neuroimage Clin. 2016;11:61–7.
21. Yucesoy K, Yuksel KZ. SCIWORA in MRI era. Clin Neurol Neurosurg. 2008;110:429–33.
22. Flanders A, Spettell CM, Tartaglino LM, Friedman DP, Herbison GJ. Forecasting motor recovery after cervical spinal cord injury: value of MR imaging. Radiology.1996;201:649–55.
23. Cohen-Adad J, El Mendili M, Lehericy S, Pradat PF, Blancho S, Rossignol S, et al. Demyelination and degeneration in the injured human spinal cord detected with diffusion and magnetization transfer MRI. Neuroimage. 2011;55:1024–33.
24. Petersen JA, Wilm BJ, von Meyenburg J, Schubert M, Seifert B, Najafi Y, et al. Chronic cervical spinal cord injury: DTI correlates with clinical and electrophysiological measures. J Neurotrauma. 2012;29:1556–66.
25. Koskinen E, Brander A, Hakulinen U, Luoto T, Helminen M, Ylinen A, et al. Assessing the state of chronic spinal cord injury using diffusion tensor imaging. J Neurotrauma. 2013;30:1587–95.
26. Kirshblum SC, Burns SP, Biering-Sorensen F, Betz R, Donovan W, Graves DE, et al. International standards for neurological classification of spinal cord injury (Revised 2011). J Spinal Cord Med. 2011;34:535–46.
27. Saksena S, Alizadeh M, Middleton DM, Conklin CJ, Krisa L, Flanders A, et al. Characterization of spinal cord diffusion tensor imaging metrics in clinically asymptomatic pediatric subjects with incidental congenital lesions. Spinal Cord Ser Cases. 2018;4:41.
28. Finsterbusch J. Improving the performance of diffusion-weighted inner field-of-view echo-planar imaging based on 2D-selective radiofrequency excitations by tilting the excitation plane. J Magn Reson Imaging. 2012;35:984–92.
29. Middleton DM, Mohamed FB, Barakat N, Hunter LN, Shellikeri S, Finsterbusch J, et al. An investigation of motion correction algorithms for pediatric spinal cord DTI in healthy participants and individuals with spinal cord injury. Magn Reson Imaging. 2014;32:433–9.
30. Chang LC, Jones DK, Pierpaoli C. RESTORE: Robust estimation of tensors by outlier rejection. Magn Reson Med. 2005;53:1088–95.
31. Ren J, Zeng G, Ma YJ, Chen N, Chen Z, Ling F, et al. Pediatric thoracic SCIWORA after back bend during dance practice: a retrospective case series and analysis of trauma mechanisms. Childs Nerv Syst. 2017;33:1191–8.
32. Vedantam A, Jirjis MB, Schmit BD, Wang MC, Ulmer JL, Kurpad SN. Diffusion tensor imaging of the spinal cord: insights from animal and human studies. Neurosurgery. 2014;74:1–8.
33. Budde MD, Kim JH, Liang HF, Schmidt RE, Russell JH, Cross AH, et al. Toward accurate diagnosis of white matter pathology using diffusion tensor imaging. Magn Reson Med. 2007;57:688–95.

ACKNOWLEDGEMENTS

We thank Rebecca Sinko, OTR/L, OTD for her help with participant recruitment and data collection.

AUTHOR CONTRIBUTIONS

Conceived and designed the analysis: SF, SS, LK, DM, MA, AF, FM. Collected the data: SF, SS, LK, DM, MA, MJ, FM. Contributed data or analysis tools: SF, SS, MA, DM, FM. Performed the analysis: SF, SS. Wrote the paper: SF, SS, LK, DM, MA, AF, KT, MJM, FB. Other contribution: JF - designed the MR sequence.

FUNDING

NIH -RO1 NSO79635-01A1 Mulcahey and Mohamed –co-PIs.

COMPETING INTERESTS

The authors declare no competing interests.

ETHICS APPROVAL AND CONSENT TO PARTICIPATE

This study was approved by the Thomas Jefferson University institutional review board (16 F.577). We certify that all applicable institutional and governmental regulations concerning the ethical use of human volunteers were followed during the course of this research.

ADDITIONAL INFORMATION

Correspondence and requests for materials should be addressed to Scott H. Faro.

Reprints and permission information is available at http://www.nature.com/reprints

Publisher's note Springer Nature remains neutral with regard to jurisdictional claims in published maps and institutional affiliations.